Available online at www.sciencedirect.com
SCIENCE DIRECT®
Journal of Computational Physics 192 (2003) 231–243
JOURNAL OF COMPUTATIONAL PHYSICS
www.elsevier.com/locate/jcp

Integral–differential equations approach to atomic three-body systems

Renat A. Sultanov [a,*], Dennis Guster [b]

[a] Department of Chemistry, University of Nevada Las Vegas (UNLV), 4505 Maryland Parkway, Box 454003, Las Vegas, NV 89154-4003, USA
[b] St. Cloud State University, Business Computing Research Laboratory (BCRL), St. Cloud, MN 56301, USA

Received 4 June 2002; accepted 8 July 2003

Abstract

Three-charge-particle quantum systems with arbitrary masses are treated by a general formalism based on a coordinate-space integral–differential Faddeev–Hahn-type equation. To solve these equations we expand the wave function components in terms of bound states in initial and final channels and project these equations on these bound states as in the close-coupling method used in Schrödinger equation. After a proper angular momentum projection, a set of coupled integral–differential equations for the unknown expansion coefficients result, which are solved numerically by discretization for the calculation of both bound state and rearrangement scattering. In this work the formalism is employed to study atomic and muonic three-body systems like negative ion of positronium $Ps^- = (e^+e^-e^-)$, positive ion of hydrogen molecule H_2^+, muonic molecules dtμ and ddμ, and also low-energy charge-transfer reaction for muonium production. Satisfactory results are obtained for all these cases. Comparison with results of other works and details of the numerical scheme are presented.

Keywords: Few-body Coulomb systems; Faddeev–Hahn-type equation; Close-coupling-approximation

1. Introduction

The quantum-mechanical few-body problem plays an important role in modern physics by providing an adequate description of few-particle systems with Coulomb, nuclear and Coulomb and nuclear forces. Its importance is derived from the fact that there are a wide range of applications in atomic and molecular physics, plasma physics, nuclear physics and astrophysics that still pose a challenge for theorists, see e.g. [1–4]. Methods developed in this field are based on detailed few-body equations which provide a correct description of the quantum few-body dynamics.

* Corresponding author.
E-mail addresses: sultano2@unlv.edu (R.A. Sultanov), dguster@stcloudstate.edu (D. Guster).

0021-9991/$ - see front matter © 2003 Elsevier B.V. All rights reserved.
doi:10.1016/j.jcp.2003.07.002

It is common knowledge that except in only a few selected systems the three-body problem cannot be solved in an explicit way. Thus developing new stable numerical schemes and effective computer algorithms are still much needed processes in the field. In quantum three-body problems the Faddeev equations [5] are the most rigorous attempt to provide a basis for numerical calculations. Although the Faddeev technique is widely used in nuclear physics that is not the case in three-body Coulomb systems.

Recently, a few-body quantum-mechanical descriptions of charge-transfer reactions within modified Faddeev equations, specifically, Faddeev–Hahn (FH) equations, have been formulated [7]. In this previous study a close-coupling method was applied, which led to the expansion of the system's wave function components into eigenfunctions of the subsystem (target) Hamiltonians providing us with a set of one-dimensional integral–differential equations after partial-wave projection was applied. It was demonstrated that the FH-equation approach is an effective tool for description of Coulomb three-body systems. So, therefore, in the current paper we will apply the method to other few-body problems and will present the numerical and computing details of the calculations. We show that our numerical scheme allows us to carry out fairly accurate calculations for various atomic three-body systems at different energies in the framework of unified computer code.

In this work we carry out calculations for: (1) ground-state energies of a negative ion of positronium $Ps^- = (e^-e^+e^-)$, where e^-/e^+ are electron/positron, respectively; a positive ion of hydrogen molecule H_2^+ and also (2) a spectrum of muonic molecules: $dt\mu^-$ and $dd\mu^-$, where d and t are hydrogen isotopes deuteron and triton, respectively, and μ^- is negative muon, (3) cross-sections of the s-wave elastic scattering of muonic hydrogen ($t\mu^-$) on deuteron d, which is one of the most important problems of muon catalyzed fusion cycle [8,9], and (4) cross-sections of the low energy muonium (Mu) production in collisions of μ^+ and hydrogen atoms, where $Mu = (\mu^+, e^-)$ represents the bound state of a positive muon and an electron. Such processes have been of interest in theory, see for example [10,11] and recent experiments [12].

The next section presents symbolic notations for three-body systems and the integral–differential equations suitable for numerical calculations. Section 3 includes details of our numerical method and the implemented algorithm. Section 4 contains tables with results and concluding remarks.

In the electronic case we use $e = \hbar = m_e = 1$, in the muonic case the units are $e = \hbar = m_\mu = 1$.

2. Integral–differential equations

Consider a Coulomb three-body system with positive charges 1 and 2, and a negative 3. Let $\vec{r}_\xi$ be a coordinate and m_ξ be a mass of the ξth particle ($\xi = 1, 2, 3$). Taking the system of units to be $e = \hbar = m_3 = 1$, let us introduce Jacobi coordinates

$$\vec{r}_{j3} = \vec{r}_3 - \vec{r}_j, \quad \vec{\rho}_k = \frac{\vec{r}_3 + m_j\vec{r}_j}{1 + m_j} - \vec{r}_k, \quad j \neq k = 1, 2. \tag{1}$$

In this work we consider only Coulomb interactions between the three particles. For any three Coulomb particles there are at most only two bound subsystems. This suggests a Faddeev formulation which uses only two components. A general procedure to derive such formulations was given by Hahn and Watson [13]. In this approach the three-body wave function is represented as follows:

$$\Psi = \Psi_1(\vec{r}_{23}, \vec{\rho}_1) + \Psi_2(\vec{r}_{13}, \vec{\rho}_2), \tag{2}$$

where each Faddeev-type component is determined by its own Jacobi coordinates. $\Psi_1(\vec{r}_{23}, \vec{\rho}_1)$ is quadratically integrable over the variable $\vec{r}_{23}$ and $\Psi_2(\vec{r}_{13}, \vec{\rho}_2)$ over the variable $\vec{r}_{13}$. To define Ψ_l ($l = 1, 2$) a set of two coupled Faddeev–Hahn-type equations can be written as

$$(E - H_0 - V_{23}(\vec{r}_{23}))\Psi_1(\vec{r}_{23}, \vec{\rho}_1) = (V_{23}(\vec{r}_{23}) + V_{12}(\vec{r}_{12}))\Psi_2(\vec{r}_{13}, \vec{\rho}_2), \tag{3}$$

$$(E - H_0 - V_{13}(\vec{r}_{13}))\Psi_2(\vec{r}_{13}, \vec{\rho}_2) = (V_{13}(\vec{r}_{13}) + V_{12}(\vec{r}_{12}))\Psi_1(\vec{r}_{23}, \vec{\rho}_1). \tag{4}$$

Here, H_0 is the kinetic energy operator of the three-particle system, $V_{ij}(r_{ij})$ are paired Coulomb interaction potentials ($i \neq j = 1, 2, 3$) and E is the total energy.

The constructed equations satisfy the Schrödinger equation exactly. For the energies below the three-body break-up threshold they have the same advantages as the Faddeev equations, because they are formulated for the wave function components with correct physical asymptotes. The Faddeev decomposition avoids overcompleteness problems because two-body subsystems are treated in an equivalent way and the correct asymptotics are guaranteed. This approach simplifies the solution procedure and provides the correct asymptotic behavior of the solution below the three-body break-up threshold.

In the general case a component of the three-body wave function has the asymptotic form which includes all open channels: elastic/inelastic, transfer and breakup [14]. In this work we shall use an approximation [15], where each component of the total wave function corresponds just to one definite channel: for the elastic/inelastic channel

$$\Psi_1(\vec{r}_{23}, \vec{\rho}_1) \underset{\rho_1 \to +\infty}{\sim} e^{ik_1 z}\varphi_1(\vec{r}_{23}) + \sum_n^{\infty} A_n^{\mathrm{el/ex}}(\Omega_{\rho_1}) \frac{e^{ik_n \rho_1}}{\rho_1} \varphi_n(\vec{r}_{23}) \tag{5}$$

and for the transfer channel

$$\Psi_2(\vec{r}_{13}, \vec{\rho}_2) \underset{\rho_2 \to +\infty}{\sim} \sum_m^{\infty} A_m^{\mathrm{tr}}(\Omega_{\rho_2}) \frac{e^{ik'_m \rho_2}}{\rho_2} \varphi_m(\vec{r}_{13}), \tag{6}$$

it is easy to see that the asymptotic behaviour of the total wave function becomes similar to Merkuriev's asymptotic [14]. Such an approximation allows us to simplify the solution procedure [16–18] and simultaneously provide a correct asymptotic behaviour of the solution before the three-body break-up threshold.

Let us delineate Eqs. (3) and (4) in terms of the adopted notations

$$\left[E + \frac{\nabla^2_{\vec{\rho}_k}}{2M_k} + \frac{\nabla^2_{\vec{r}_{j3}}}{2\mu_j} - V_{j3}\right]\Psi_k(\vec{r}_{j3}, \vec{\rho}_k) = (V_{j3} + V_{jk})\Psi_j(\vec{r}_{k3}, \vec{\rho}_j). \tag{7}$$

Here $j \neq k = 1, 2$ and $\mu_j^{-1} = 1 + m_j^{-1}$. We are using the Jacobi coordinates

$$\vec{\rho}_j = \vec{r}_{j3} - \beta_k \vec{r}_{k3}, \quad \vec{r}_{j3} = \frac{1}{\gamma}(\beta_k \vec{\rho}_k + \vec{\rho}_j) \quad \text{and} \quad \vec{r}_{jk} = \frac{1}{\gamma}(\sigma_j \vec{\rho}_j - \sigma_k \vec{\rho}_k), \tag{8}$$

with the following mass-coefficients: $\beta_k = m_k/(1 + m_k)$, $\sigma_k = 1 - \beta_k$ and $\gamma = 1 - \beta_k\beta_j$. To solve (7) we expand the wave function components in terms of bound states in initial and final channels and project this equation on these bound states. The same approach has been used in the framework of the cluster reduction method in nuclear physics [19].

The expansion of the wave function is given by

$$\Psi_k(\vec{r}_{j3}, \vec{\rho}_k) \approx \sum_{LM\lambda l} \sum_n \frac{1}{\rho_k} f_{nl\lambda}^{(k)LM}(\rho_k) R_{nl}^{(k)}(r_{j3}) \left\{ Y_\lambda(\hat{\vec{\rho}}_k) \otimes Y_l(\hat{\vec{r}}_{j3}) \right\}_{LM}, \tag{9}$$

where $\alpha \equiv (nl\lambda)$ are quantum numbers of a three-body state and L is the total angular momentum of the three-body system obtained by coupling l and λ, Y_{lm}s are the spherical harmonics, $R_{nl}^{(k)}(r_{j3})$ is the radial part of the hydrogen-like bound-state wave function, $f_{nl\lambda}^{(k)LM}(\rho_k)$ are the unknown expansion coefficients. This

prescription is similar to that adopted in the close-coupling approximation. After a proper angular momentum projection, the set of integral–differential equations for the unknown expansion functions $f^{(k)}_{nl\lambda}(\rho_k)$ can be written as

$$\left[\left(k_n^{(1)}\right)^2+\frac{\partial^2}{\partial\rho_1^2}-\frac{\lambda(\lambda+1)}{\rho_1^2}\right]f_\alpha^{(1)}(\rho_1)=g_1\sum_{\alpha'}\frac{\sqrt{(2\lambda+1)(2\lambda'+1)}}{2L+1}\int_0^\infty \mathrm{d}\rho_2 f_{\alpha'}^{(2)}(\rho_2)$$
$$\times\int_0^\pi \mathrm{d}\omega\sin\omega R_{nl}^{(1)}(|\vec{r}_{23}|)\left[-\frac{1}{|\vec{r}_{23}|}+\frac{Z_1}{|\vec{r}_{12}|}\right]R^{(2)}_{n'l'}(|\vec{r}_{13}|)\rho_1\rho_2$$
$$\times\sum_{mm'}D^L_{mm'}(0,\omega,0)C^{Lm}_{\lambda 0lm}C^{Lm'}_{\lambda' 0l'm'}Y^*_{lm}(v_1,\pi)Y_{l'm'}(v_2,\pi), \tag{10}$$

$$\left[\left(k_n^{(2)}\right)^2+\frac{\partial^2}{\partial\rho_2^2}-\frac{\lambda'(\lambda'+1)}{\rho_2^2}\right]f_\alpha^{(2)}(\rho_2)=g_2\sum_{\alpha'}\frac{\sqrt{(2\lambda+1)(2\lambda'+1)}}{2L+1}\int_0^\infty \mathrm{d}\rho_1 f_{\alpha'}^{(1)}(\rho_1)$$
$$\times\int_0^\pi \mathrm{d}\omega\sin\omega R_{nl}^{(2)}(|\vec{r}_{13}|)\left[-\frac{Z_1}{|\vec{r}_{13}|}+\frac{Z_1}{|\vec{r}_{12}|}\right]R^{(1)}_{n'l'}(|\vec{r}_{23}|)\rho_2\rho_1$$
$$\times\sum_{mm'}D^L_{mm'}(0,\omega,0)C^{Lm}_{\lambda 0lm}C^{Lm'}_{\lambda' 0l'm'}Y^*_{lm}(v_2,\pi)Y_{l'm'}(v_1,\pi). \tag{11}$$

Here, $g_k=4\pi M_k/\gamma^3$, $k_n^{(i)}=\sqrt{2M_i(E-E_n^{(j)})}$, with $M_i^{-1}=m_i^{-1}+(1+m_j)^{-1}$, $E_n^{(j)}$ is the binding energy of $(j3)$, $i\neq j=1,2$, $\gamma=1-m_km_j/((1+m_k)(1+m_j))$, $D^L_{mm'}(0,\omega,0)$ the Wigner function, $C^{Lm}_{\lambda 0lm}$ the Clebsh–Gordon coefficient, ω is the angle between the Jacobi coordinates $\vec{\rho}_i$ and $\vec{\rho}_{i'}$, v_i is the angle between $\vec{r}_{i'3}$ and $\vec{\rho}_i$, $v_{i'}$ is the angle between $\vec{r}_{i3}$ and $\vec{\rho}_{i'}$. The following relations are useful for a numerical treatment $\sin v_i=(\rho_{i'}/\gamma r_{i'3})\sin\omega$ and $\cos v_i=(1/\gamma r_{i'3})(\beta_i\rho_i+\rho_{i'}\cos\omega)$ $(i\neq i'=1,2)$.

To find a unique solution to (10) and (11), appropriate boundary conditions, depending upon the specific situation, need to be considered. First we impose

$$f_\alpha^{(1)}(\rho_1)\underset{\rho_1\to 0}{\sim}f_{\alpha'}^{(2)}(\rho_2)\underset{\rho_2\to 0}{\sim}0. \tag{12}$$

(1) To calculate three-body bound states we impose vanishing boundary conditions:

$$f_\alpha^{(1)}(\rho_1)\underset{\rho_1\to+\infty}{\sim}f_{\alpha'}^{(2)}(\rho_2)\underset{\rho_2\to+\infty}{\sim}0. \tag{13}$$

(2) For the three-body scattering problem, say $(13)+2\to 2+(13)$, we impose "standing wave" boundary condition:

$$f_{1s}^{(1)}(\rho_1)\underset{\rho_1\to+\infty}{\sim}\sin(k_1^{(2)}\rho_1)+\tan\delta_0\cos(k_1^{(2)}\rho_1), \tag{14}$$

where δ_0 is the scattering phase shift and the cross-section is

$$\sigma_{\mathrm{el}}=(\sqrt{4\pi}/k_1^{(2)}\sin\delta_0)^2. \tag{15}$$

(3) Finally, for the three-body charge-transfer problems we apply the well known K-matrix formalism [20]. This method has already been applied for solution of three-body problems in the framework of the coordinate-space Faddeev–Merkuriev equations [6]. For the present scattering problem with $1+(23)$ as the initial state, in the asymptotic region, it takes two solutions to (10) and (11) satisfy the following boundary conditions:

$$\begin{cases} f_{1s}^{(1)}(\rho_1) \underset{\rho_1\to+\infty}{\sim} \sin(k_1^{(1)}\rho_1) + K_{11}\cos(k_1^{(1)}\rho_1), \\ f_{1s}^{(2)}(\rho_2) \underset{\rho_2\to+\infty}{\sim} \sqrt{v_1/v_2}K_{12}\cos(k_1^{(2)}\rho_2), \end{cases} \tag{16}$$

where K_{ij} are the appropriate coefficients. For scattering with $2+(13)$ as the initial state, we impose the following conditions:

$$\begin{cases} f_{1s}^{(1)}(\rho_1) \underset{\rho_1\to+\infty}{\sim} \sqrt{v_2/v_1}K_{21}\cos(k_1^{(1)}\rho_1), \\ f_{1s}^{(2)}(\rho_2) \underset{\rho_2\to+\infty}{\sim} \sin(k_1^{(2)}\rho_2) + K_{22}\cos(k_1^{(2)}\rho_2), \end{cases} \tag{17}$$

where v_i $(i = 1, 2)$ are velocities in channel i. With the following change of variables in (10) and (11)

$$\begin{aligned} \mathrm{f}_{1s}^{(1)}(\rho_1) &= f_{1s}^{(1)}(\rho_1) - \sin(k_1^{(1)}\rho_1), \\ \mathrm{f}_{1s}^{(2)}(\rho_2) &= f_{1s}^{(2)}(\rho_2) - \sin(k_1^{(2)}\rho_2), \end{aligned} \tag{18}$$

we obtain two sets of inhomogeneous equations which are solved numerically. The coefficients K_{ij} are obtained from the numerical solution of the Faddeev–Hahn-type equations. The cross-sections are given by

$$\sigma_{ij} = \frac{4\pi}{k_1^{(i)2}} \frac{\delta_{ij}D^2 + K_{ij}^2}{(D-1)^2 + (K_{11}+K_{22})^2}, \tag{19}$$

where $i, j = 1, 2$ refer to the two channels and $D = K_{11}K_{22} - K_{12}K_{21}$.

3. Numerical method

For numerical solution of the set of coupled integro-differential equations (10) and (11) we apply the discretization method [21]. On the right-hand side of the equations the integrals over ρ_1 and ρ_2 are replaced by sums using the trapezoidal rule and the second-order partial derivatives on the left-hand side are discretized using a three-point rule [22]. By this means we get a set of linear equations for the unknown coefficients $f_\alpha^{(i)}(k)$ $(k = 1, N_p)$:

$$\left[k_n^{(1)2} + D_{ij}^2 - \frac{\lambda(\lambda+1)}{\rho_{1i}^2}\right] f_\alpha^{(1)}(i) - \frac{M_1}{\gamma^3}\sum_{\alpha'=1}^{N_s}\sum_{j=1}^{N_p} w_j S_{\alpha\alpha'}^{(12)}(\rho_{1i},\rho_{2j}) f_{\alpha'}^{(2)}(j) = 0, \tag{20}$$

$$-\frac{M_2}{\gamma^3}\sum_{\alpha=1}^{N_s}\sum_{j=1}^{N_p} w_j S_{\alpha'\alpha}^{(21)}(\rho_{2i},\rho_{1j}) f_\alpha^{(1)}(j) + \left[k_{n'}^{(2)2} + D_{ij}^2 - \frac{\lambda'(\lambda'+1)}{\rho_{2i}^2}\right] f_{\alpha'}^{(2)}(i) = B_{\alpha'}^{21}(i). \tag{21}$$

Here, coefficients w_j are weights of the integration points ρ_{1i} and ρ_{2i} $(i = 1, N_p)$, N_s is the number of quantum states which are taken into account in the expansion (9). This is a well known close-coupling approximation method in atomic physics [20]. In this work we use up to 10 states, that is five atomic states 1s–2s–2p–3s–3p in each centrum. D_{ij}^2 is the three-point numerical approximation of the second-order differential operator:

$$D_{ij}^2 f_\alpha(i) = \frac{f_\alpha(i-1)\delta_{i-1,j} - 2f_\alpha(i)\delta_{i,j} + f_\alpha(i+1)\delta_{i+1,j}}{\Delta}, \tag{22}$$

where Δ is a step of the grid $\Delta = \rho_{i+1} - \rho_i$. The vector $B_{\alpha'}^{21}(i)$ is

$$B^{(21)}_{\alpha'}(i) = \frac{M_2}{\gamma^3}\sum_{j=1}^{N_p} w_j S^{(21)}_{\alpha' 1so}(i,j)\sin(k_1\rho_j), \tag{23}$$

and in symbolic-operator notations the set of linear equations (21) has the following form:

$$\sum_{\alpha'=1}^{2*N_s}\sum_{j=1}^{N_p} \mathbf{A}_{\alpha\alpha'}(i,j)\vec{f}_{\alpha'}(j) = \vec{b}_{\alpha}(i). \tag{24}$$

The discretized equations are subsequently solved by the Gauss elimination method [23]. As can be seen from Eqs. (20) and (21) the matrix **A** has a block structure. There are four main blocks in the matrix: two of them related to differential operators and other two to integral operators. Each of these blocks has sub-blocks depending on the quantum numbers $\alpha = nl\lambda$ and $\alpha' = n'l'\lambda'$. The second-order differential operators produce three-diagonal sub-matrices. In Fig. 1 the structure of the matrix **A** is presented.

There is no need to keep the whole matrix **A** in the computer's RAM. The following optimization strategy shows that one can reduce memory usage at least four times. Actually, the numerical equations (20) and (21) can be written in the following way:

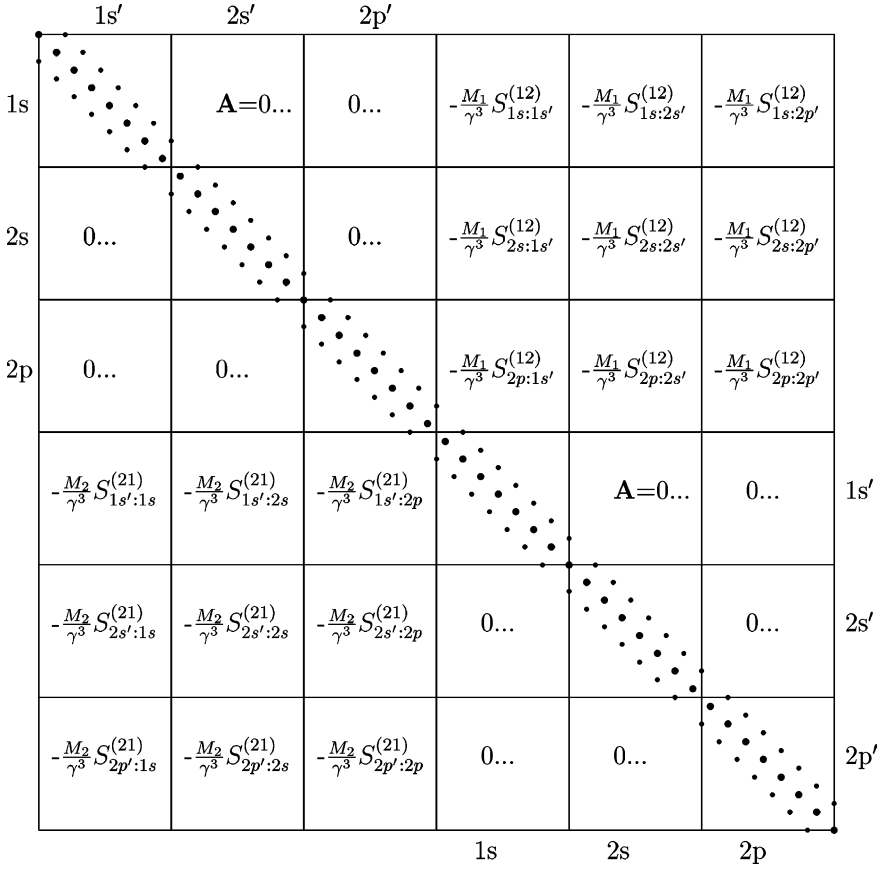

Fig. 1. Structure of the block-matrix **A**.

$$D_1 f^1 - \frac{M_1}{\gamma^3} S^{12} f^2 = 0, \tag{25}$$

$$-\frac{M_2}{\gamma^3} S^{21} f^1 + D_2 f^2 = b. \tag{26}$$

Here, D_1, D_2, S^{12} and S^{21} are submatrixes of **A**. From Eq. (25) one can determine that

$$f^1 = (D_1)^{-1} M_1 / \gamma^3 S^{12} f^2, \tag{27}$$

where $(D_1)^{-1}$ is reverse matrix of D_1. Finally, we obtain a reduced set of linear equations which are used to perform the calculations

$$\left[D_2 - \frac{M_1 M_2}{\gamma^6} S^{21} (D_1)^{-1} S^{12} \right] f^2 = b. \tag{28}$$

To solve the integral–differential equations, one has to calculate the angular integrals in Eqs. (10) and (11) which are independent of the energy E. One needs to calculate them only once and store them on hard disk for the later calculation of other observables, for instance, the cross-sections at different energies. Subintegrals in Eqs. (10) and (11) have strong dependence on ρ_i and $\rho_{i'}$. To calculate $S^{(ii')}_{\alpha\alpha'}(\rho_i, \rho_{i'})$ at different coordinates an adaptable algorithm has been used [23]. In this case using the relation

$$\cos\omega = \frac{x^2 - \beta_i^2 \rho_i^2 - \rho_{i'}^2}{2\beta_i \rho_i \rho_{i'}}, \tag{29}$$

the angle dependent part of the equations can be written now as the following integral:

$$S^{(ii')}_{\alpha\alpha'}(\rho_i, \rho_{i'}) = \frac{4\pi}{\beta_i} \frac{[(2\lambda+1)(2\lambda'+1)]^{1/2}}{2L+1} \int_{|\beta_i\rho_i - \rho_{i'}|}^{\beta_i\rho_i + \rho_{i'}} \mathrm{d}x R^{(i)}_{nl}(x) \times \left[-1 + \frac{x}{r_{ii'}(x)} \right] R^{(i')}_{n'l'}(r_{i3}(x)) \times \sum_{mm'} D^L_{mm'}(0, \omega(x), 0) C^{Lm}_{\lambda 0 lm} C^{Lm'}_{\lambda' 0 l'm'} Y_{lm}(v_i(x), \pi) Y^*_{l'm'}(v_{i'}(x), \pi). \tag{30}$$

Note that the expression (30) differs from zero only in a narrow strip when $\rho_i \approx \rho_{i'}$, because for the considered three-body systems the coefficient β_i is approximately equal to one. This fact is demonstrated in Figs. 2 and 3, where we present as examples selected angle integral surfaces (30): $S^{(12)}_{2s:2p'}(\rho_1, \rho_2)$ and $S^{(21)}_{2s':2s}(\rho_2, \rho_1)$ for $\mu^+e^-p^+$ three-body system. All angle integral surfaces have pretty different forms. In order to obtain a converged solution we needed a large number of discretization points (up to 1000) adequately distributed between 0 and 40–60 atomic/muonic units. More points are taken near the origin where the interaction potentials are large; a smaller number of points are needed at large distances.

It is easy to estimate the total amount N_Q of angle integrals $S^{(ii')}_{\alpha\alpha'}(\rho_i, \rho_{i'})$ which are needed to fill out the matrix **A**, Fig. 1. For example, in the case of $N_p = 1000$ discretization points and 10-state approximation $N_s = 2 \times 5$: $N_Q = 5 \times N_s \times N_p \times N_p \sim 10^8$. However in view of the fact that the value of $S^{(ii')}_{\alpha\alpha'}(\rho_i, \rho_{i'})$ is mostly concentrated in the narrow strip, when $\rho_i \approx \rho_{i'}$ one can reduce N_Q by factor $\sim 10^{-4}$. We shall discuss the results and details of calculations in next section.

In this work we deal with various Coulomb three-body systems at different energies. For a specific physical situation described by the set of second-order integral–differential equations (10) and (11) one has to impose specific boundary conditions to the equations. For example, to calculate bound states of a Coulomb three-body system we have to impose two boundary conditions (12) and (13). Taking into account the structure of the second-order differential operator D^2_{ij} (22) these conditions can be easily

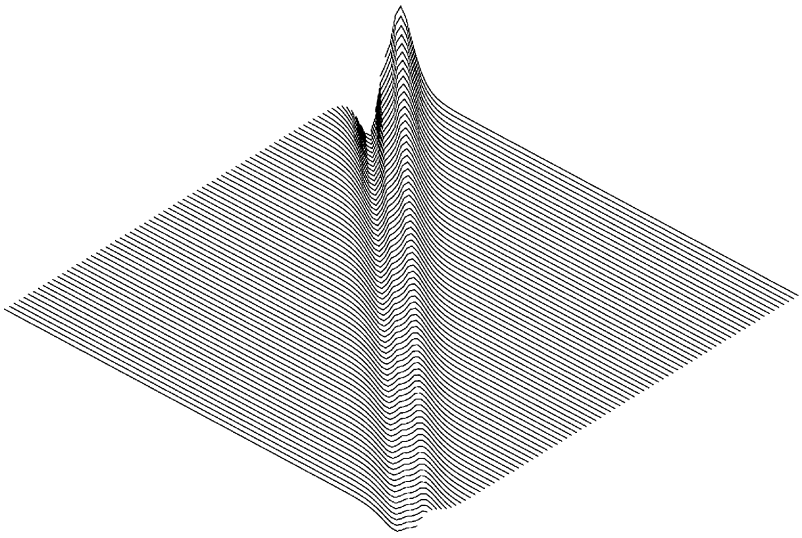

Fig. 2. $S^{(12)}_{2s;2p'}(\rho_1,\rho_2)$ function for $\mu^+e^-p^+$ system.

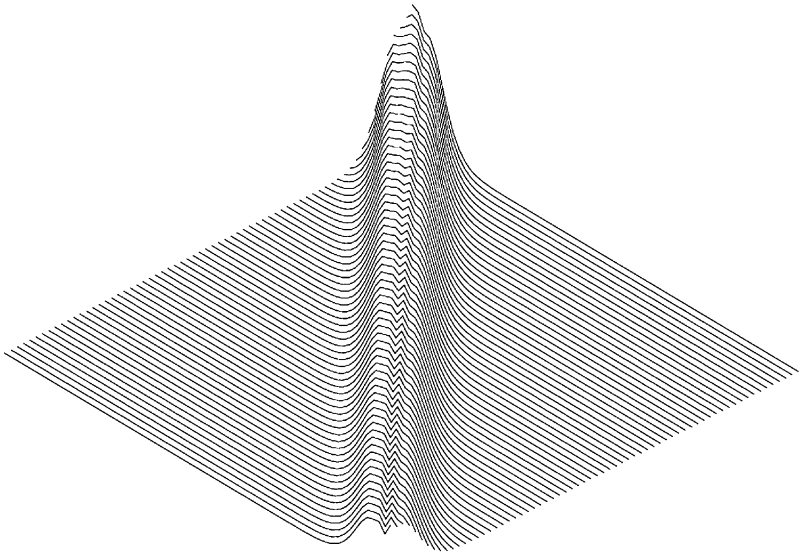

Fig. 3. $S^{(21)}_{2s';2s}(\rho_2,\rho_1)$ function for $\mu^+e^-p^+$ system.

incorporated into the matrix **A**. For example, from Fig. 1 one can see that for the first line of the matrix $i = 1$ and for line with $i = N_p$

$$f(0) = 0 \quad \text{and} \quad f(N_p + 1) = 0, \tag{31}$$

these values verify that the conditions (12) and (13) are satisfied automatically. To calculate binding energies $E_b(\xi)$ $(\xi = 1, 2, \ldots)$ of a three-body system we get $\vec{b}_\alpha(i) = 0$. The linear set (24) has a solution when the determinant of the matrix **A** is equal to zero, that is

$$\det[\mathbf{A}_{ij}(E_b(\xi))] = 0, \tag{32}$$

where $E_b(\xi)$ are unknown parameters. In the case of scattering (14) and rearrangement scattering (16) and (17) problems we apply almost the same procedure and also have to use Eq. (18).

The computer code is constructed in such a way so that it can be applied to various three-body atomic problems without major changes. For different quantum systems we need only to correctly input muonic/atomic units, masses of particles, their charges and appropriate boundary conditions. Our computer code consists of three main parts: (1) initialization of data and numerical grid; (2) calculation of the angular integrals $S_{\alpha\alpha'}(\rho_1, \rho_2)$ (30) and saving them on the computer's hard disk; (3) construction of the main matrix **A** using the $S_{\alpha\alpha'}(\rho_{1i}, \rho_{2j})$, solution of the set of linear equations, production of the three-body wave function and, finally, the calculation of physical observables, for the given example's cross-sections. All these tasks are implemented into the unique computer code.

4. Results

1. In this work we apply the Faddeev–Hahn integral–differential equations approach and the numerical algorithm and computation procedure described in Section 3 to quantum three-body systems with pure Coulomb interactions and *arbitrary* masses. At first we calculate ground-state energies of some atomic systems. In Table 1 we present our results within the 6-state $2 \times$ (1s–2s–2p) and the 10-state $2 \times$ (1s–2s–2p–3s–3p) approximations to the close-coupling expansion (9) together with the results of recent variational calculations, which are considered to be the most accurate to date. We carried out calculations for a negative ion of positronium Ps^- and a positive ion of a hydrogen molecule H_2^+.

It has been demonstrated herein for Ps^- and H_2^+ systems that the Faddeev–Hahn method is able to produce results within ~11% in the 6-state model and ~3.5% in the 10-state model calculations. Convergent numbers are obtained in these cases with up to 900 points of integration which we distributed between 0 and $40a_0$, where a_0 is the radius of the hydrogen atom.

2. Now we consider muonic systems, which are of interest in the muon catalyzed fusion cycle of thermonuclear reactions (cold fusion) [8]. First we deal with the spectrum level of muonic molecules. The spectrum of muonic molecules $dt\mu^-$ and $dd\mu^-$ has also been calculated in the 10-state approximation which takes into account the quantum states with $n \leqslant 3$ and $n' \leqslant 3$ as well as orbital quantum numbers over the $\vec{r}_{j3} : l \leqslant 1$, $l' \leqslant 1$ and $\vec{\rho}_k : \lambda \leqslant 1$, $\lambda' \leqslant 1$. Obtained results are listed in Table 2. The following values of masses (in the units of the electron mass m_e) have been used in the calculations: muon mass is $m_\mu = 206.769$; deuteron mass $m_d = 3670.481$ and triton mass $m_t = 5496.918$.

In order to obtain converged results we needed a large number of integration points (up to 900) adequately distributed between 0 and $50a_\mu$, where a_μ is the radius of the muonic hydrogen. More points are taken near the origin where the interaction potentials are large. A small number of points are needed at large distances. For example, near the origin we took up to 40 equally spaced points per unit length interval a_μ, in the intermediate region ($\rho = 10$–$20a_\mu$) we took up to 15 equally spaced points per unit length interval a_μ. In Table 2 we also present the results of variational calculations [26] which are considered to be the most

Table 1
Results for ground-state energies of Ps^- and H_2^+ in atomic units

Atomic systems	Faddeev–Hahn equations		Other results
	1s–2s–2p model	1s–2s–2p–3s–3p model	
Ps^-	−0.30	−0.27	−0.2620051 [24]
H_2^+	−0.66	−0.62	−0.597139 [25]

Table 2
Spectrum level of muonic molecules, eV

Muonic molecules	Faddeev–Hahn equations		Variational results [26]
	1s–2s–2p model [15]	1s–2s–2p–3s–3p model	
dtμ	−323.1	−319.4	−319.1397
dtμ*	−32.9	−33.7	−34.8345
ddμ	−326.4	−325.2	−325.0735
ddμ*	−33.1	−35.0	−35.8444

accurate in the literature. The values of binding energies are counted out from the ground level of a mesoatom having the heaviest nucleus given in eV. The excited states are denoted by the asterisk. We obtain very good agreement with the variational calculations. Here, we would like to point out that all considered problems above, namely Ps^-, H_2^+, $dt\mu^-$ and $dd\mu^-$, represent useful examples of three-body Coulomb systems for testing and comparison of different methods. For these systems we have also calculated their wave functions.

The advantage of our method is that it is general in nature and is applicable to a variety of systems. To achieve this flexibility we sacrifice a degree of precision. We can calculate beyond 3–4 digits, but in doing so do not get stable results. Our current level of stability provides results that are within ~1.5–3.5% of the known quantities generated by their respective specific algorithm.

3. To provide an example of three-body elastic scattering problem we calculated the results of the following process:

$$(t\mu)_{1s} + d \to d + (t\mu)_{1s} \tag{33}$$

below the $(t\mu)_{n=2}$ threshold. This collision has generated great interest in the context of resonance formation of muonic molecules $dt\mu^-$ in the muon catalyzed fusion cycle. The structure of our computer code allows us to reuse the angular integrals (30) calculated earlier when we determined the spectrum level of the $dt\mu^-$ system. However, for the scattering problem (for the open channel) we need to impose different boundary equations, namely (12) and (14). In Table 3 we include our results from the 6-state approximation and also the results of [6], which were performed using the three-dimensional Faddeev–Merkuriev coordinate-space approach and results of multilevel adiabatic calculations [9]. As can be seen, our results are in reasonable agreement with results of works [6,9]. We have found that for this process the low energy scattering phase shift δ_0 (see expressions (14) and (15)) was rather sensitive to different numerical parameters of our calculations such as the number of integration points and the maximum value of the inte-

Table 3
S-wave elastic cross-sections σ_{el} (10^{-19} cm^2) for $(t\mu)_{1s} + d$ scattering

Energy E (eV)	Faddeev–Hahn equations (1s–2s–2p model)	3D-Faddeev–Merkuriev equations [6]	Adiabatical approach [9]
40.0	0.4	0.371	–
30.0	0.7	0.636	–
20.0	1.1	1.072	–
10.0	2.0	1.763	1.9
5.0	2.5	–	2.4
3.0	2.7	–	2.5
1.0	2.3	2.158	2.4
0.5	2.2	1.975	2.2
0.3	2.1	–	2.1
0.1	1.7	1.628	1.7

gration $\rho_{\max}$. We had to integrate up to $\rho_{\max} \approx 100$ atomic (muonic) units for this system and got stable results only in two digits. The same approximation in the standard close-coupling treatment (static exchange approximation) is well known to be not satisfactory.

4. In this work we carry out analysis of a three-body charge-exchange reaction, namely e^- transfer, for a muonium Mu formation in collision of positive muons μ^+ with hydrogen atoms H at low energies

$$\mu^+ + H_{1s} \to Mu_{1s} + p^+, \tag{34}$$

where p^+ is a proton. Here, we would like to point out that the muonium atom Mu is an ultralight isotope of hydrogen: $m(H)/m(Mu) \approx 9$. Investigation of these atoms may provide an exceptionally sensitive probe of dynamical mass effects in physical chemistry and chemical physics. Current areas of interest are in μ^+ charge exchange and Mu-formation (34) as well as chemical reaction in collisions of Mu with H_2 molecules [27,28]. The most interesting energies for laboratory investigations are low-energy collisions.

Our cross-sections σ_{ex} for Mu-formation (34) are presented in Fig. 4 together with the theoretical results of work [11]. We employ atomic units: distances are measured in units of a_0. In solving this problem distances up to $60a_0$ were considered and 900–1000 points were used in the discretization. The following mass values are used in the unit of electron mass: $m_p = 1836.152$ and $m_{\mu^+} = 206.769$.

Because we are mainly concerned with the very low-energy collisions $E_{col} \sim 10^{-2}$–10^{-4} eV we employed only the lowest partial wave $L = 0$. The value of E_{col} is counted out from the ground level of the hydrogen atom H_{1s} and the momenta $k^{(1)}$ and $k^{(2)}$ in Eqs. (10) and (11) are

$$k^{(2)} \approx \sqrt{\frac{2m_p m_\mu}{m_p + m_\mu} E_{col}}, \quad k^{(1)} \approx \sqrt{(k^{(2)})^2 + \frac{m_p - m_\mu}{m_p + m_\mu}}. \tag{35}$$

It is shown that our 6-state model calculations for $\sigma_{ex}(k^{(2)})$, where $k^{(2)} \approx 3.7 \times \sqrt{E_{col}\ (eV)}$, generally reproduce for low energies the behaviour of the same cross-section from work [11]. We found that the

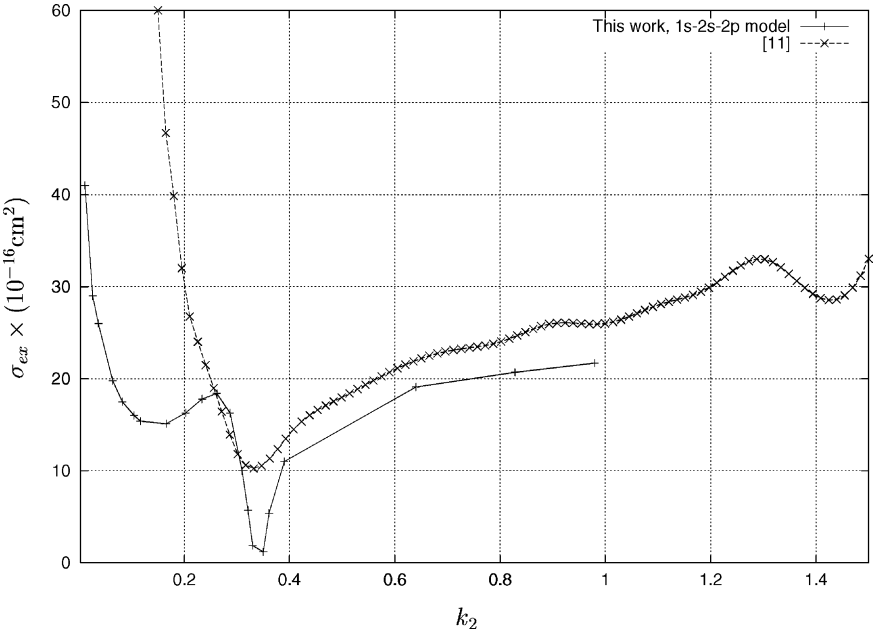

Fig. 4. Cross-section of the reaction $\mu^+ + H_{1s} \to Mu_{1s} + p^+$.

contribution of p-waves in sub-systems is reasonable and ranges up to 20–40%. It would be useful for future work to extend the basis in the expansion (9) and obtain converged results as was done in our previous calculations for binding energies of atomic and muonic three-body systems (presented in Tables 1 and 2 of this work).

5. Conclusion

The study of three-body Coulomb problems has been the subject of this work. We have investigated different atomic and muonic three-body systems in the framework of a detailed few-body approach. It was shown that the method of using Faddeev–Hahn equations (3) and (4) and close-coupling approximation is effective and able to produce with 10- or even only 6-states in the close-coupling expansion results that are accurate within ~11% in the 1s–2s–2p model and ~3.5% in the 1s–2s–2p–3s–3p model, respectively not just for binding energies of atomic three-body systems (Table 1), but for muonic molecules (Table 2), three-body elastic scattering (Table 3) and charge-transfer reactions (Fig. 4) as well. We constructed an effective algorithm, which allows us to considerably conserve computer resources. The whole procedure leads to a great reduction of the usual technical effort and is definitely worth being considered. Additionally, we are committed to further increasing the efficiency of this computer code by employing a variety of parallel processing techniques in both loosely coupled and tightly coupled environments [29,30].

Acknowledgements

The algorithm described herein has been selected for inclusion in a parallel processing optimization project at the BCRL. We thank St. Cloud State University, MN for providing computing resources for this project. Partial support of this research was also provided by NSF Grant No. ATM-0205199.

References

[1] T. Yamazaki, N. Morita, R.S. Nayano, E. Widmann, J. Eades, Phys. Rep. 366 (2002) 183.
[2] E. Nielsen, D.V. Fedorov, A.S. Jensen, E. Garrido, Phys. Rep. 347 (2001) 374.
[3] R.A. Sultanov, S.K. Adhikari, J. Phys. B 35 (2002) 935;
Phys. Lett. A 300 (4–5) (2002) 417.
[4] A.G. Abrashkevich, M.S. Kaschiev, S.I. Vinitsky, J. Comp. Phys. 163 (2000) 328.
[5] L.D. Faddeev, Sov. Phys. JETP 12 (1961) 1014.
[6] A.A. Kvitsinsky, C.-Y. Hu, J.S. Cohen, Phys. Rev. A 53 (1996) 255.
[7] R.A. Sultanov, S.K. Adhikari, Phys. Rev. A 61 (2000) 022711.
[8] P. Ackerbauer et al., Nucl. Phys. A 652 (1999) 331.
[9] V.S. Melezhik, L.I. Ponomarev, M.P. Faifman, Sov. Phys. JETP 58 (1983) 254.
[10] R.K. Janev, Dz.S. Belkic, J. Phys. B 5 (1972) L237.
[11] A.V. Matveenko, J. Phys. B 10 (1977) 1133.
[12] L.D.A. Siebbeles, S.M. Pimblott, S.F.J. Cox, J. Chem. Phys. 111 (1999) 7493.
[13] Y. Hahn, K.M. Watson, Phys. Rev. A 5 (1972) 1718.
[14] S.P. Merkuriev, Ann. Phys. NY 130 (1980) 395.
[15] R.A. Sultanov, in: H. Horiuchi, Y. Fujiwara, M. Matsuo, M. Kamimura, H. Toki, Y. Sakuragi (Eds.), Innovative Computational Methods in Nuclear Many-Body Problems, World Scientific, Singapore, 1998, pp. 131–135.
[16] A.M. Mukhamedzhanov, R.A. Sultanov, J. Phys. B 25 (1992) 5263.
[17] R.A. Sultanov, Few-Body Syst. Suppl. 10 (1999) 281.
[18] R.A. Sultanov, S.K. Adhikari, J. Phys. B 32 (1999) 5751.
[19] I.N. Filikhin, S.L. Yakovlev, Phys. Atom. Nucl. 63 (2000) 336.

[20] N.F. Mott, H.S.W. Massey, The Theory of Atomic Collisions, Clarendon Press, London, 1965.
[21] R.L. Burden, J.D. Faires, Numerical Analysis, seventh ed., Brooks/Cole Publishing Company, 2000.
[22] M. Abramowitz, I.A. Stegun, Handbook of Mathematical Functions, National Bureau of Standards, 1964.
[23] W.H. Press, B.P. Flannery, S.A. Teukolsky, W.T. Vetterling, Numerical Recipes in C: The Art of Scientific Computing, The Press Syndicate of the University of Cambridge, Cambridge, 1992.
[24] A.M. Frolov, Phys. Rev. A 57 (1998) 2436.
[25] R.E. Moss, J. Phys. B 32 (1999) L89.
[26] S.A. Alexander, H.J. Monkhorst, Phys. Rev. A 38 (1988) 26.
[27] M. Senba, D.G. Fleming, D.J. Arseneau, H.R. Mayne, J. Chem. Phys. 112 (2000) 9390.
[28] K. Tsuda, K. Moribayashi, H. Nakamura, J. Chem. Phys. 103 (1995) 5512.
[29] D. Guster, R.A. Sultanov, J.Q. Chen, Information Technology and Organizations: Trends, Issues, Challenges and Solutions, Mehdi Khosrow-Pour, Information Resources Management Association, USA, Idea Group Publishing, 2003, pp. 165–167.
[30] R.A. Sultanov, D. Guster, Lect. Notes Comput. Sci. 2667 (2003) 568.